Intense laser field effect on the nonlinear optical properties of triple quantum wells consisting of parabolic and inverse-parabolic quantum wells

O Ozturk[1,*], B O Alaydin[2,3], D Altun[3,4] and E Ozturk[2]

[1] Department of Nanotechnology Engineering, Sivas Cumhuriyet University, Sivas, Turkiye
[2] Department of Physics, Sivas Cumhuriyet University, Sivas, Turkiye
[3] Nanophotonics Research and Application Center, Sivas Cumhuriyet University, Sivas, Turkiye
[4] Department of Electricity and Energy, Sivas Vocational School, Sivas Cumhuriyet University, Sivas, Turkiye

E-mail: ozanozturk@cumhuriyet.edu.tr

CrossMark

Abstract

The nonlinear optical rectification, the second harmonic generation coefficient, and the third harmonic generation coefficient in parabolic-inverse parabolic-parabolic quantum wells (PIPPQWs) and inverse parabolic-parabolic-inverse parabolic quantum wells (IPPIPQWs) are calculated varying the intense laser field (ILF) parameter (α_0). The modifications of the dipole moment matrix elements and the energy levels are depending on the potential shape. The results show that the ILF intensity exerts an active influence on the profile, height, and width of the confinement potential of both PIPPQW and IPPIPQW. The potential profile of IPPIPQW has been affected otherwise than PIPPQW for different ILF intensities. The nonlinear optical rectification, the second harmonic generation, and the third harmonic generation coefficients of PIPPQW and IPPIPQW could be altered in the energy range and the size of the resonance peak by rising the ILF intensity. By changing the α_0 parameter, it is conceivable to organize red or blue shift at the resonance peak positions of the nonlinear optical rectification, the second harmonic generation, and the third harmonic generation coefficients. The shift of the nonlinear optical rectification coefficient occurs when the difference between the ground and the second energy levels changes. According to the parameters used here, while for PIPPQW the spectrum of the resonance peak of the nonlinear optical rectification displays a blue shift with increasing ILF, this spectrum displays a red shift for IPPIPQW. The consequences can be valued in investigating new ways of changing the optical and electronic properties of semiconductor quantum wells.

Keywords: intense laser field, parabolic quantum well, inverse parabolic quantum well, electro-optical changes, nonlinear optical rectification, second harmonic generation, third harmonic generation

(Some figures may appear in colour only in the online journal)

---

* Author to whom any correspondence should be addressed.

1. Introduction

The quantum wells, which contain largely non-homogeneous parts rather than having a rectangular profile, have obtained increasing attention due to their various applications. Such structures provide the desired optical properties for device design which can be used to modulate and control the intensity output of semiconductor devices. By varying potential well shape, both the energy levels and the wave function change, and accordingly a large number of physical features modify. For example, the parabolic quantum wells have been used as a cascade barrier part of the quantum well lasers to develop the optical limiting parameter and as a collection of carriers to a thin quantum well to decrease the threshold current density [1, 2]. The parabolic quantum wells exhibit unique physical properties that are of interest from theoretical and practical perspectives. The parabolic quantum wells are also used to reflect infrared detectors with low leakage current [3] and are used in resonance tunneling devices for potential claims in high-speed circuits [4]. Theoretical and experimental research on the influences of magnetic, electric, and laser fields and the hydrostatic pressure in the parabolic quantum wells [5–13] and the inverse parabolic quantum wells [12–15] have also been the topic of attention in most investigates.

The linear and nonlinear optical developments connected to the intersubband transitions in low-dimensional semiconductor systems have enticed extensive consideration because of the strong quantum confinement conclusion, leading to minor energy separation between the energy levels, the great importance of dipole moment matrix elements (DMMEs), and the possibility of realizing resonance situations. Consequently, the linear and nonlinear optical properties have been widely investigated in low-dimensional semiconductor structures due to device application potentials in the infrared region of the electromagnetic spectrum. The DMMEs show that semiconductor quantum wells have a large nonlinearity. For the nonlinear optical properties of low-dimensional semiconductor structures, it is very important to investigate the second and third-order nonlinearities. Recently, some authors have studied nonlinear optical rectification, the second harmonic generation, and the third harmonic generation coefficients in low-dimensional semiconductors [16–21].

The intense laser field (ILF) effects on the confinement potential and the corresponding energy levels play a vital role in optoelectronic device demonstrating. The influence of ILF with high-frequency also causes significant changes in the form of the confinement quantum well potential [22–26], and transition from the single quantum well potential to double quantum well potential can be achieved by the ILF effect [23]. As the potential profile of the system is strongly tuned with the ILF parameter (α_0), the optical characteristics, as well as energy states change significantly. The rapid convergence of exciting levels in GaAlAs/GaAs quantum well with increasing ILF density allows improving population inversion in the optical pumping scheme, which is important for the design of powerful quantum well lasers. Therefore, we consider that it is worth considering the effect of ILF on the nonlinear optical properties for different quantum well structures.

The non-resonant ILF intensity can be used as a way to utilize the electronic and optical properties of the quantum wells. Since GaAlAs/GaAs structures are useful in modern photoelectronic and high-speed electronic devices, pressure and external field dependence of electrical and optical properties in related systems have been widely considered [27–31].

We consider $Ga_{1-x}Al_xAs/GaAs$ structure with parabolic-inverse parabolic-parabolic quantum wells (PIPPQWs) and inverse parabolic-parabolic-inverse parabolic quantum wells (IPPIPQWs). In this study, theoretical studies of the nonlinear optical rectification, the second harmonic generation, and the third harmonic generation coefficients of PIPPQW and IPPIPQW by rising ILF are emphasized. To the best of our knowledge, this is the first research article, which compares these nonlinear optical properties in PIPPQW and IPPIPQW structures.

2. Theory

The wave functions and corresponding energy levels of PIPPQW and IPPIPQW can be calculated by solving the Schrödinger equation under effective mass approximation.

$$\left(-\frac{\hbar^2}{2m^*}\frac{d^2}{dz^2} + V(z) \right)\Psi(z) = E\Psi(z). \tag{1}$$

Herein, $V(z)$ symbolizes the confinement potential, and E and $\Psi(z)$ correspond to the eigenenergy and eigenfunction. The confinement potential of PIPPQW and IPPIPQW (L_L, L_M, L_R are the left, middle, right quantum well widths) have taken as

$$V^{PIPPQW}(z)$$
$$= V_0 \begin{cases} \frac{2}{L_L^2}\left(z + \left(\frac{L_L + L_M}{2}\right)\right)^2 & -\left(L_L + \frac{L_M}{2}\right) \leqslant z \leqslant -\frac{L_M}{2} \\ -\frac{2}{L_M^2}\left(z^2\right) + \frac{1}{2} & -\frac{L_M}{2} \leqslant z \leqslant \frac{L_M}{2} \\ \frac{2}{L_R^2}\left(z - \left(\frac{L_M + L_R}{2}\right)\right)^2 & \frac{L_M}{2} \leqslant z \leqslant \left(\frac{L_M}{2} + L_R\right) \\ 1 & \text{elsewhere} \end{cases}$$
$$\tag{2a}$$

$$V^{IPPIPQW}(z)$$
$$= V_0 \begin{cases} -\frac{2}{L_L^2}\left(z + \left(\frac{L_L + L_M}{2}\right)\right)^2 + \frac{1}{2} & -\left(L_L + \frac{L_M}{2}\right) \leqslant z \leqslant -\frac{L_M}{2} \\ \frac{2}{L_M^2}\left(z^2\right) & -\frac{L_M}{2} \leqslant z \leqslant \frac{L_M}{2} \\ -\frac{2}{L_R^2}\left(z - \left(\frac{L_M + L_R}{2}\right)\right)^2 + \frac{1}{2} & \frac{L_M}{2} \leqslant z \leqslant \left(\frac{L_M}{2} + L_R\right) \\ 1 & \text{elsewhere} \end{cases}$$
$$\tag{2b}$$

The Floquet method has been used to combine the non-resonant polarized ILF effect through the z-direction [32].
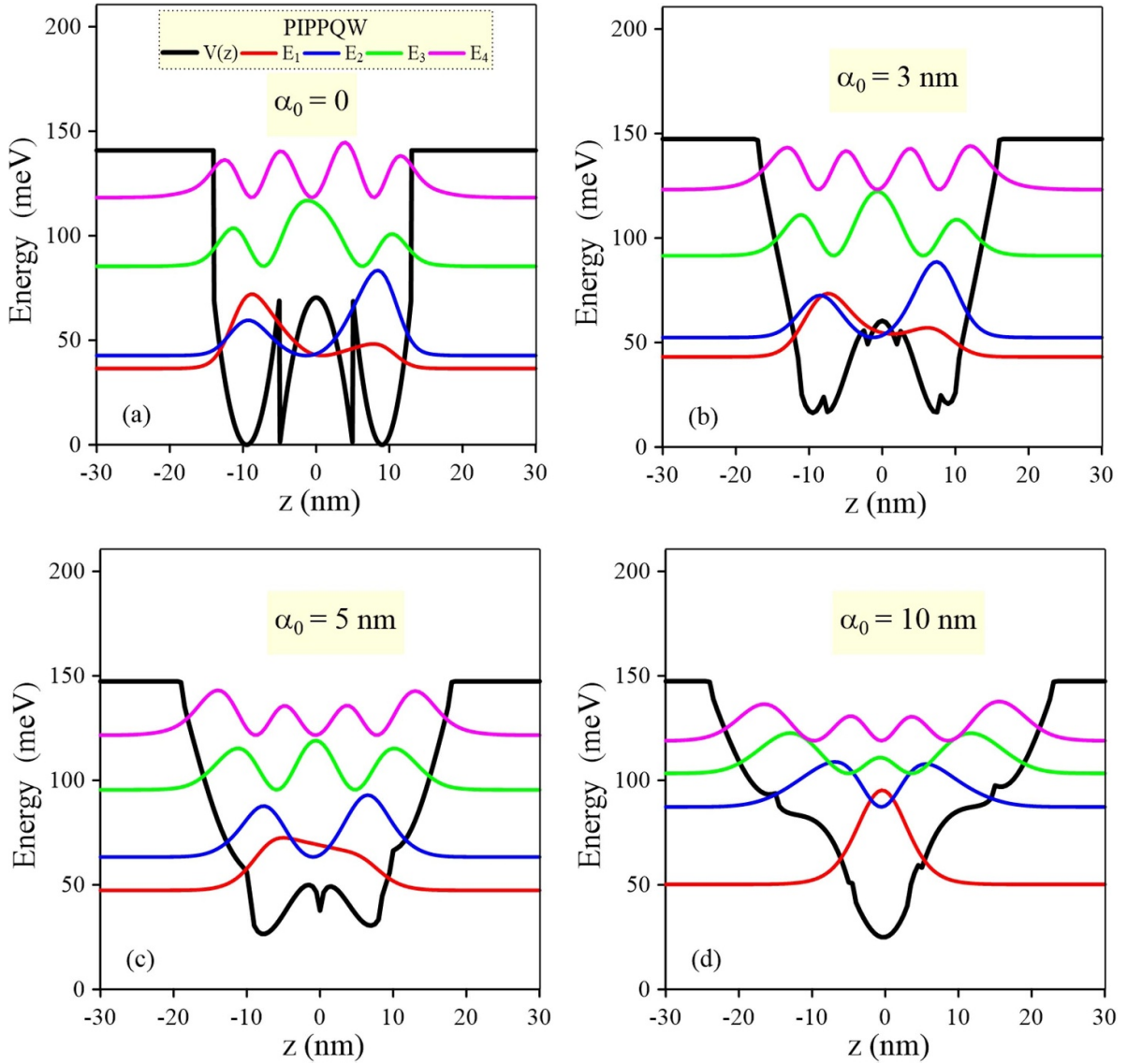
Figure 1. For PIPPQW the confinement potential profile (black curve) and the squared wave functions related to the first four energy levels for (a) $\alpha_0 = 0$, (b) $\alpha_0 = 3$ nm, (c) $\alpha_0 = 5$ nm, (d) $\alpha_0 = 10$ nm.

In the high-frequency regime [33, 34], a closed-form for the dressed potential is offered. Hence, the second term at the left-hand side in equation (1) should be recovered by $V(z) \rightarrow \langle V(z, \alpha_0) \rangle$. The laser-dressed potentials are presented by [34]:

$$\langle V(z, \alpha_0) \rangle = \frac{\Omega}{2\pi} \int_0^{2\pi/\Omega} V(z + \alpha_0 \sin \Omega t)\, dt \qquad (3)$$

where $\alpha_0 = \sqrt{\frac{e^2 8\pi I_{\text{laser}}}{m^{*2} c \Omega^4}}$ is the laser-dressing parameter [26, 35], I_{laser} is the mean intensity of the laser, c is the light velocity, and Ω is the laser frequency.

After the wave functions and corresponding energy levels are obtained, the nonlinear optical rectification [17, 19], the second harmonic generation [18, 19], and the third harmonic generation [18, 19] coefficients have been given under the compact density matrix approach as in equations (4)–(6);

$$\chi_0^{(2)} = \frac{4e^3 \sigma_v}{\varepsilon_o} M_{21}^2 \delta_{21}$$

$$\times \frac{E_{21}^2 \left(1 + \frac{\Gamma_2}{\Gamma_1}\right) + \hbar^2 \left(\omega^2 + \Gamma_2^2\right)\left(\frac{\Gamma_2}{\Gamma_1} - 1\right)}{\left((E_{21} - \hbar\omega)^2 + (\hbar\Gamma_2)^2\right)\left((E_{21} + \hbar\omega)^2 + (\hbar\Gamma_2)^2\right)} \qquad (4)$$

$$\chi_{2\omega}^{(2)} = \frac{e^3 \sigma_v}{\varepsilon_o} \frac{M_{21} M_{32} M_{31}}{(\hbar\omega - E_{21} - i\hbar\Gamma_3)(2\hbar\omega - E_{31} - i\hbar\Gamma_3/2)} \qquad (5)$$
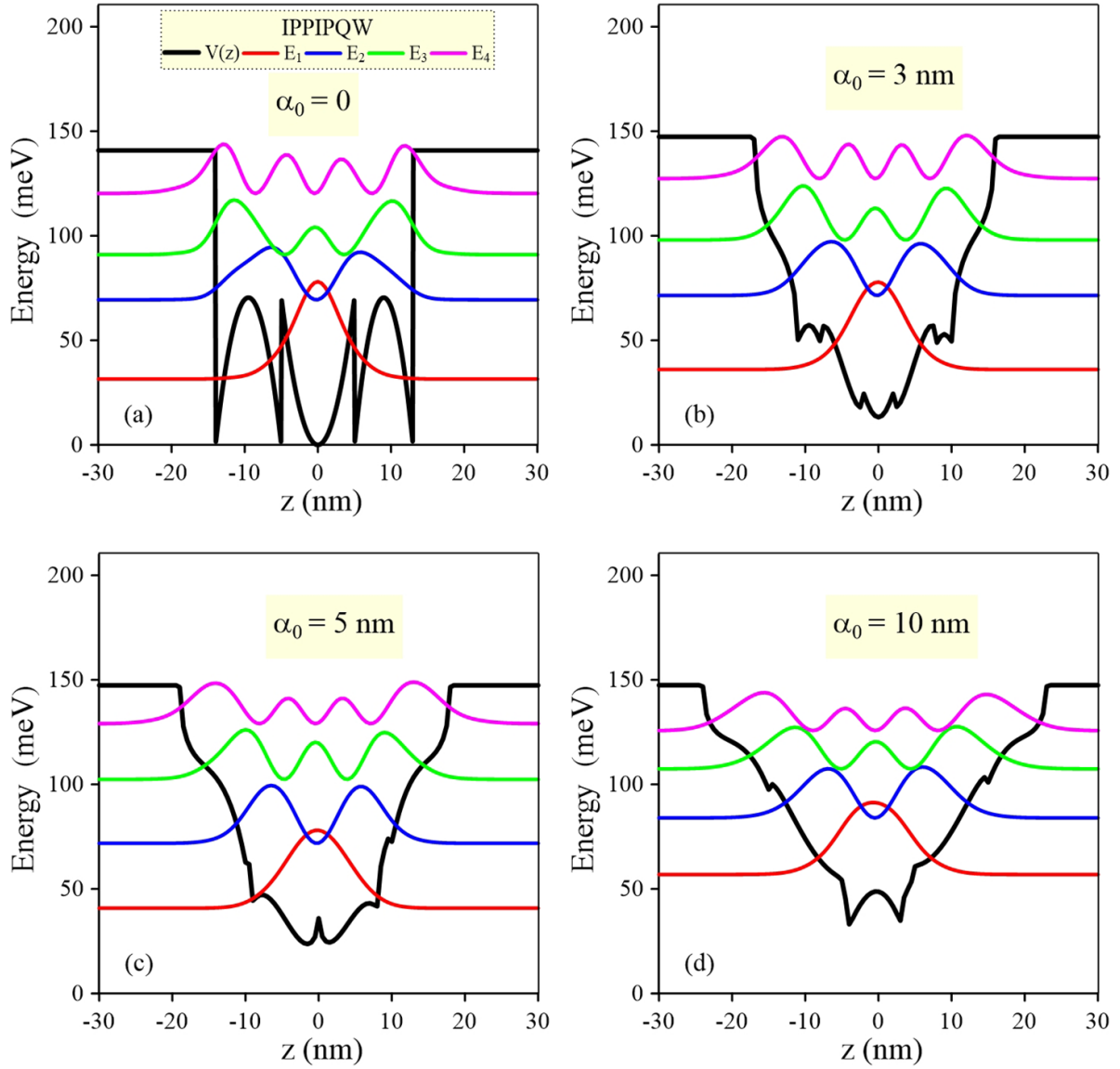
Figure 2. For IPPIPQW the confinement potential profile (black curve) and the squared wave functions related to the first four energy levels for (a) $\alpha_0 = 0$, (b) $\alpha_0 = 3$ nm, (c) $\alpha_0 = 5$ nm, (d) $\alpha_0 = 10$ nm.

$$\chi_{3\omega}^{(3)} = \frac{e^4 \sigma_v}{\varepsilon_o} \frac{M_{21} M_{32} M_{43} M_{41}}{(\hbar\omega - E_{21} - i\hbar\Gamma_3)(2\hbar\omega - E_{31} - i\hbar\Gamma_3/2)(3\hbar\omega - E_{41} - i\hbar\Gamma_3/3)}. \tag{6}$$

M_{fi} describes the DMMEs and it is given as

$$M_{fi} = \int \Psi_f^* z \Psi_i dz , \ (i,f = 1,2,3,4) \tag{7}$$

where the angular frequency of the photon is represented as ω, $(E_{fi} = E_f - E_i = \hbar\omega_{fi})$, E_f and E_i are the final and initial energy states, $\delta_{21} = M_{22} - M_{11}$ is the intrasubband DMME, ε_o is the vacuum permittivity, and σ_v is carrier density.

3. Results and discussion

We have investigated the nonlinear optical rectification, the second harmonic generation, and the third harmonic generation coefficients in PIPPQW and IPPIPQW with and without ILF. In this study, $m^* = 0.067 m_0$, $L_L = 9$ nm, $L_M = 10$ nm, $L_R = 8$ nm, $V_0 = 148$ meV ($V_0 = 0.6 (1.155x + 0.37x^2)$ (eV), for $x = 0.2$), $T_1 = 1/\Gamma_1 = 1$ ps, $T_2 = 1/\Gamma_2 = 0.5$ ps, $\hbar/T_3 = \hbar\Gamma_3 = 0.5$ meV, $\sigma_v = 5 \times 10^{22} \text{m}^{-3}$.

For several α_0 intensities, the confined potential profiles and the squared of the wave functions corresponding to the bounded states of PIPPQW and IPPIPQW are presented in figures 1 and 2, seriatim. It is seen that the shape, width, height of the effective well, the energy levels, and the wave functions in PIPPQW and IPPIPQW have changed strongly with increasing α_0 value. As the ILF intensity is applied, the bottom of the potential profiles of PIPPQW and IPPIPQW shifts upwards. When the ILF is increased more ($\alpha_0 > L/2$), the shape of the whole potential profile changes. The energy levels values in IPPIPQW have been obtained differently from PIP-PQW, with and without the ILF. It is noticed from these figures that both potential shape and energy levels of PIPPQW are more sensitive to the α_0 value. For $\alpha_0 = 0 (\alpha_0 = 5 \text{ nm})$, the energy levels of PIPPQW occurs at 36, 42, 85, and 118 meV (47, 63, 95, and 121 meV), respectively, whereas the energy levels of IPPIPQW are observed at 31, 69, 90, and 120 meV (40, 71, 102 and 129 meV), respectively. As seen obviously in figures, the most remarkable change happens in the ground energy level of IPPIPQW. Also, the biggest change in PIPPQW is seen in the ground and second energy levels. These differences between the ground and second energy levels are seen in figure 3(a) and table 1. When the ILF is applied, we can say that the observed variation in the potential profiles and the energy levels crucially affect the nonlinear optical properties of the structure based on intersubband transitions.

Figures 3(a)–(c) shows three energy differences, several DMMEs, and three DMME's products as a function of α_0 for PIPPQW and IPPIPQW, separately. With the increase of α_0 value, the E_{21} energy difference in PIPPQW varies greatly. As seen from figures 3(b) and (c), the minimum and maximum of both DMMEs and DMME's products depend on the α_0 parameter. The energy differences and the DMMEs are also heavily dependent on the ILF intensity for many semiconductor device applications.

For PIPPQW and IPPIPQW, figures 4(a) and (b) shows the calculated nonlinear optical rectification coefficient versus the photon energy for several α_0 values. The shift of the nonlinear optical rectification coefficient is attributed to the variation of the E_{21} value for increasing ILF. Respectively, for PIPPQW and IPPIPQW, the spectrum of the resonant peak displays a blue shift up to $\alpha_0 \leqslant 11$ nm and $\alpha_0 \leqslant 1$ nm, and then a red shift for $\alpha_0 > 11$ nm and $\alpha_0 > 1$ nm, which is related to the variation of E_{21} by rising α_0 value (see figure 3(a)). Since the shift of the resonance peak should be consistent with the change of the interval energy E_{21}, the position of the resonance peak is at $E_{21} \approx \hbar\omega$. While the spectrum of the nonlinear optical rectification in PIPPQW shows a blue shift with increasing ILF, this spectrum displays a red shift for IPPIPQW. The maxima of the nonlinear optical rectification coefficient are proportional to the DMME's product ($\left|M_{21}^2 \delta_{21}\right|$). $\left|\delta_{21}\right|$ values, which contribute to the size of the nonlinear optical rectification, are due to the presence of asymmetry in the potential profile. In figure 3(c), the DMME's product ($\left|M_{21}^2 \delta_{21}\right|$) is the maximum at $\alpha_0 = 0$ and the minimum at $\alpha_0 = 7$ nm for both PIP-PQW and IPPPQW. While the resonance peak of the nonlinear optical rectification coefficient decreases with increasing
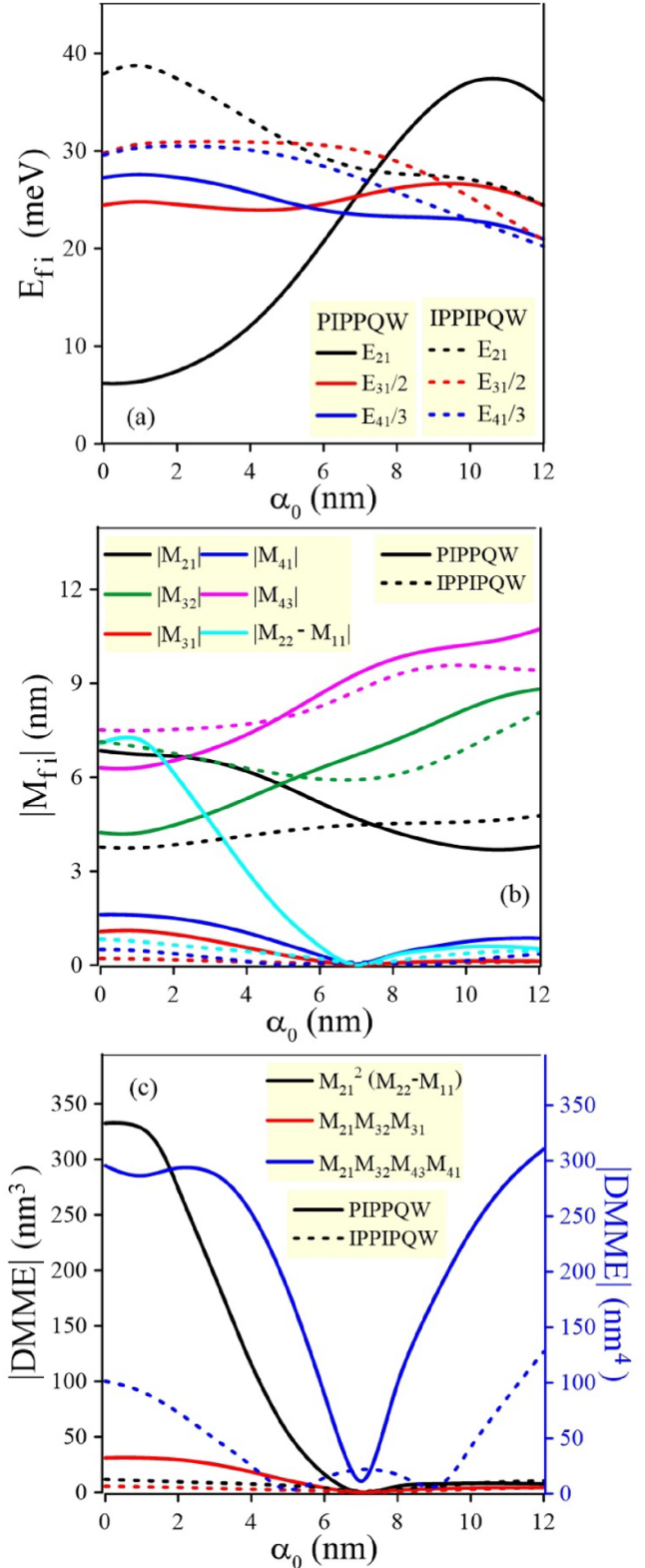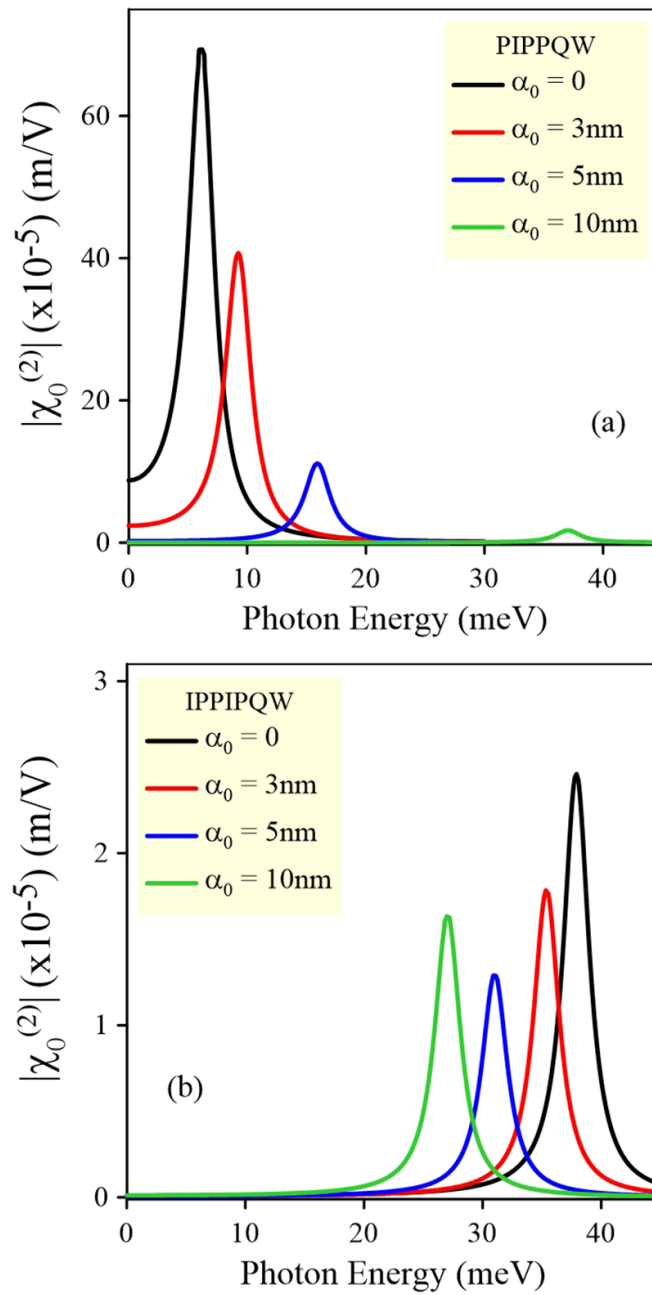

Figure 3. For PIPPQW and IPPIPQW, (a) three energy differences, (b) numerous DMMEs, and (c) DMME's product as a function of the ILF value.

ILF for PIPPQW, the size of this coefficient at $\alpha_0 = 10$ nm is greater than at $\alpha_0 = 5$ nm for IPPIPQW.

In figures 5(a) and (b), the plotted the second harmonic generation coefficients as a function of the photon energy

Table 1. For PIPPQW and IPPIPQW, the energy differences between the resonance peaks for different ILF values.

	PIPPQW			IPPIPQW		
	Energy difference (meV)			Energy difference (meV)		
0	−18.25	−2.81	−21.06	8.16	0.15	8.31
3	−14.89	−2.5	−17.39	4.44	0.53	4.97
5	−8.10	−0.69	−8.79	0.22	1.37	1.59
10	10.49	3.64	14.13	1.79	2.31	4.10

Figure 4. The nonlinear optical rectification coefficient as a function of photon energy for several ILF values for (a) PIPPQW and (b) IPPIPQW.

for PIPPQW and IPPIPQW are shown for several α_0 values. Two resonance peaks relate to each one of the resonance frequencies. The corresponding position of resonance peak is at $E_{31}/2 \approx \hbar\omega$ (dominant-major peak) and at $E_{21} \approx \hbar\omega$ (weak-minor peak). The energy difference between these two resonance peaks is offered in table 1 for different α_0 parameters. The separation of the second harmonic generation coefficients is the direct result of the asymmetrically spaced energy levels. For PIPPQW, the $E_{31}/2$ value remained almost constant up to $\alpha_0 < 6$ nm and then increased, and the largest value has been seen at $\alpha_0 = 9$ nm. Also, for IPPIPQW, the $E_{31}/2$ value remained almost constant up to $\alpha_0 < 7$ nm and then decreased, and the smallest value has been seen at $\alpha_0 = 12$ nm. Thus, the dominant peak at $\alpha_0 = 10$ nm shows the blue shift for PIPPQW and the red shift for IPPIPQW. The variations of E_{21} are the same as in the nonlinear optical rectification coefficient. As seen from figure 5 and table 1, in PIPPQW for $0 < \alpha_0 \leqslant 7$ nm range, the minor resonance peak of the second harmonic generation coefficient is to the left of the major resonance peak. Because E_{21} value is less than $E_{31}/2$ in this range. Also, for IPPIPQW the major of the resonance peak appears as a single peak because the E_{21} and $E_{31}/2$ values are almost the same for $\alpha_0 = 5$ nm. For 6 nm $\leqslant \alpha_0 \leqslant 8$ nm range, E_{21} value is less than $E_{31}/2$. Thus, according to the parameters used here, the minor resonance peak of the second harmonic generation coefficient is to the right of the major resonance peak. The magnitude of the resonance peaks of the second harmonic generation coefficient is consistent with the variations of the absolute DMME's product ($|M_{21}M_{32}M_{31}|$) and the energy differences. These DMME's product is minimum at $\alpha_0 = 7$ nm for both PIPPQW and IPPIPQW. The physical reason for these results is the change in the confinement of electrons by rising α_0 parameter.

For PIPPQW and IPPIPQW, the third harmonic generation coefficient versus the photon energy is plotted in figures 6(a) and (b) for different ILF values, separately. It is seen that three resonance peaks are observed and these peaks are corresponding to the resonance frequencies. The position of the resonance peak is at $E_{41}/3 \approx \hbar\omega$ (dominant-major peak), $E_{31}/2 \approx \hbar\omega$ (middle peak), and at $E_{21} \approx \hbar\omega$ (very weak-minor peak). For PIPPQW, all resonance peaks (except $\alpha_0 = 10$ nm) are sorted from right to left according to energy differences, respectively for $E_{41}/3$, $E_{31}/2$, and E_{21}. (For $\alpha_0 = 10$ nm this order is E_{21}, $E_{31}/2$, and $E_{41}/3$). However, for IPPIPQW, the resonance peaks are sorted from left to right according to energy differences, respectively, $E_{41}/3$, $E_{31}/2$, and E_{21}. The major resonance peak appears as a single peak because $E_{41}/3$ and $E_{31}/2$ (E_{21} and $E_{31}/2$) values are close to each other at $\alpha_0 = 0$ ($\alpha_0 = 5$ nm). The energy differences between the resonance peak s are also shown in table 1. As can be seen from this table, the energy differences of PIPPQW and IPPIPQW are very different from each other. For PIPPQW, the resonance peak spectrum of $E_{41}/3$ displays a red shift. Whereas for IPPIPQW, the spectrum gives the blue shift up to $\alpha_0 \leqslant 2$ nm and the red shift after $\alpha_0 > 2$ nm. The variations of the resonance peak spectrum of $E_{31}/2$ and E_{21} are the same as in the second harmonic generation coefficient. For PIPPQW and IPPIPQW, the variation of the DMME's product ($|M_{21}M_{32}M_{43}M_{41}|$) is
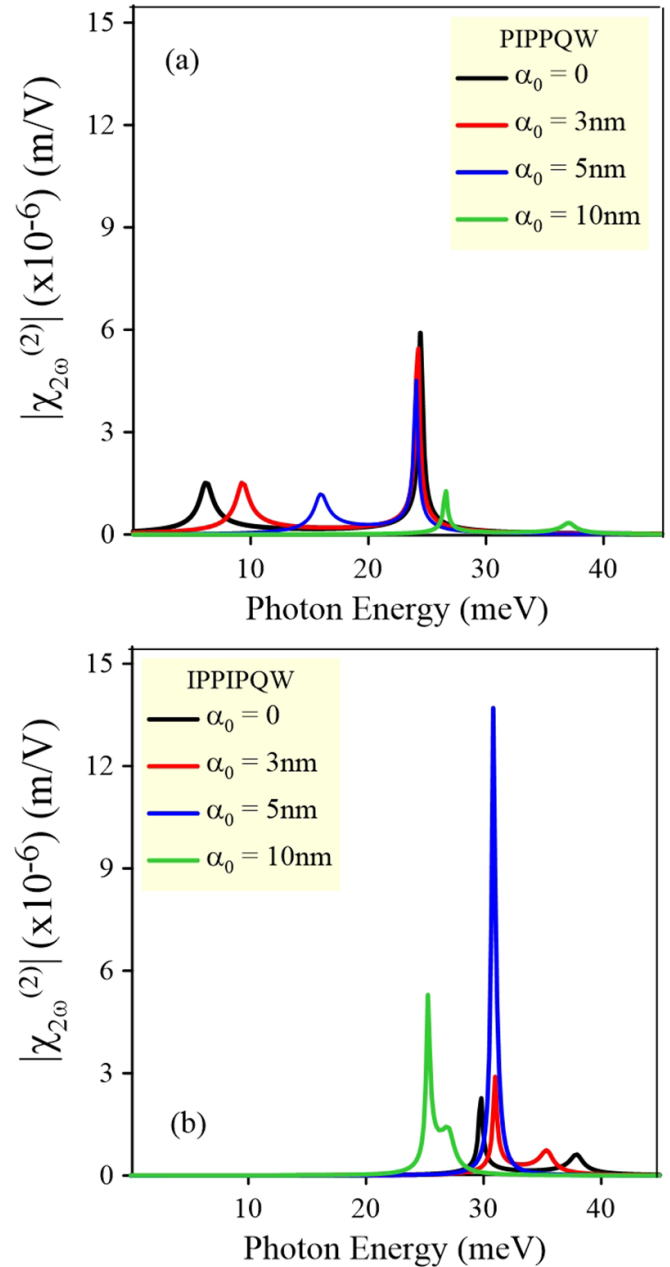

Figure 5. The second harmonic generation coefficient versus photon energy for several ILF values for (a) PIPPQW and (b) IPPIPQW.

quite different from each other. While the multiplication of the DMMEs ($|M_{21}M_{32}M_{43}M_{41}|$) is the minimum at $\alpha_0 = 7$ nm for PIPPQW, this is the minimum at $\alpha_0 = 5$ nm and $\alpha_0 = 9$ nm for IPPIPQW (see figure 3(c)). The results show that change in the resonance peak of the third harmonic generation coefficient not only directly results of the absolute product of the DMMEs $|M_{21}M_{32}M_{43}M_{41}|$, but also in the energy interval E_{21}, E_{31}, E_{41} in the denominator, which introduces more asymmetry to the system. The overlap between the wave functions varies due to the dissimilarity of potential profile geometry changed by the ILF parameter. Effects on the DMMEs are related to the behavior of the electron wave function and the geometric confinement of electrons in quantum wells.
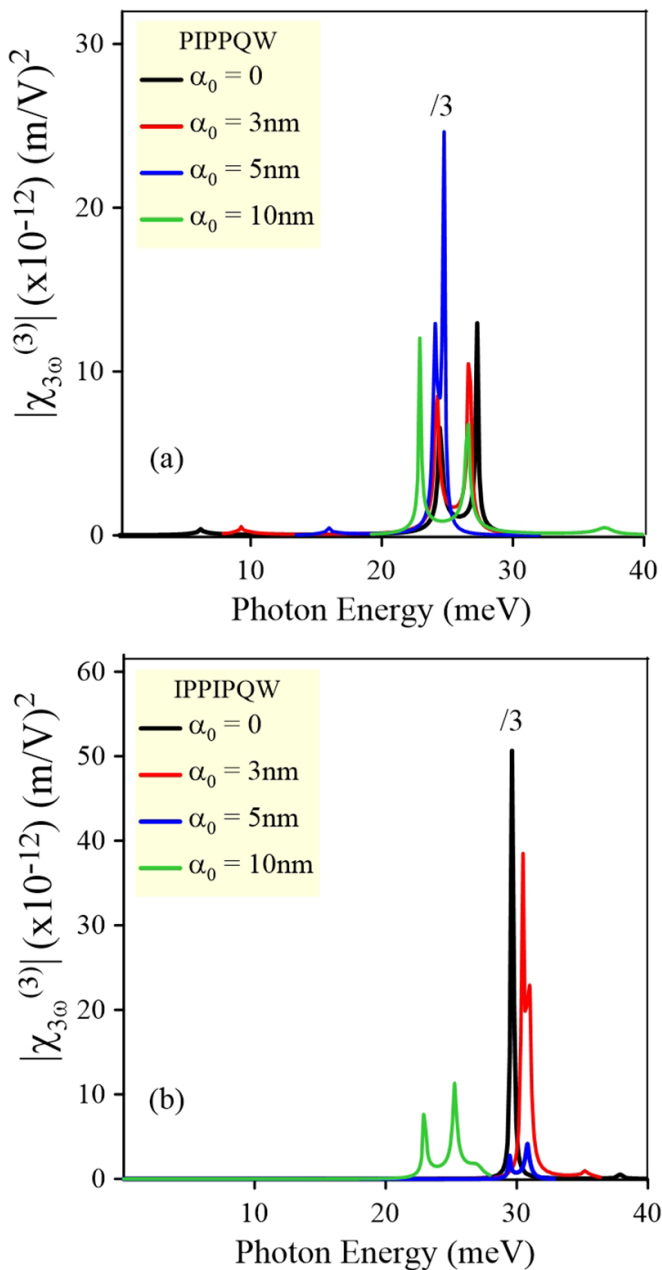
Figure 6. The third harmonic generation coefficient as a function of photon energy for several ILF values for (a) PIPPQW and (b) IPPIPQW. (Blue (a) and black (b) curves were reduced by 3 times for PIPPQW and IPPIPQW, respectively.)

4. Conclusions

Herein, the effective mass approximation is applied to solve the time-independent Schrödinger equation to obtain the wave functions and the energy levels for the PIPPQW and IPPIPQW under the ILF. For several ILF intensities, the nonlinear optical rectification, the second harmonic generation, and the third harmonic generation coefficients are calculated as a function of the incident photon energy. The ILF parameters have a huge impact on the nonlinear optical rectification, the second harmonic generation, and the third harmonic generation coefficients. The shape of the quantum wells is changed with increasing ILF density, resulting in the variation of the energy levels, the electron probability densities, and the DMMEs. This development is a way of studying how to control the electron in these systems. It has been presented that the energy separation among energy levels has varied with increasing ILF value. As the ILF intensity changes, the DMMEs are revised due to the overlap between the status wave function. We have concluded that the position and size of the resonance peaks of the nonlinear optical rectification, the second harmonic generation, and the third harmonic generation coefficients are depending on the ILF because of the change in the DMMEs and the energy difference. In a conclusion, we can say that it is possible to tune the electronic and optical features of PIP-PQW and IPPIPQW by adjusting ILF. To do that varying ILF parameters is one of the ways. The obtained numerical results are important to design PIPPQW and IPPIPQW based semiconductor devices.

References

[1] Kasemset D, Hong C S, Patel N B and Dapkus P D 1983 *IEEE J. Quantum Electron.* **QE-19** 1025
[2] Mawst L J, Givens M E, Zmudzinski C A, Emanuel M A and Colemen J J 1987 *IEEE J. Quantum Electron.* **QE-23** 696
[3] Karunasiri R P G and Wang K L 1988 *Superlattices Microstruct.* **4** 661
[4] Gossard A C, Miller R C and Wiegmann W 1986 *Surf. Sci.* **174** 131
[5] Mamani N C, Duarte C A, Gusev G M, Quivy A A and Lamas T E 2006 *Braz. J. Phys.* **36** 336
[6] Ozturk E and Sokmen I 2014 *J. Lumin.* **145** 387
[7] Radu A, Niculescu E and Cristea M 2008 *J. Optoelectron. Adv. Mater.* **10** 2555
[8] Guo K-X and Gu S-W 1993 *Phys. Rev.* B **47** 16322
[9] Niculescu E C and Burileanu L 2003 *Mod. Phys. Lett.* B **17** 1253
[10] Shu-Fang M, Yuan Q and Shi-Liang B 2018 *Chin. Phys.* B **27** 027103
[11] Wang Z P, Liang X X and Wang X 2007 *Eur. Phys. J.* B **59** 41
[12] Ozturk O, Ozturk E and Elagoz S 2019 *Phys. Scr.* **94** 115809
[13] Ozturk E 2017 *Optik* **139** 256
[14] Chen W Q, Wang S M, Andersson T G and Thordson J 1993 *J. Appl. Phys.* **74** 6247
[15] Baskoutas S, Garoufalis C and Terzis A F 2011 *Eur. Phys. J.* B **84** 241
[16] Karimi M J and Keshavarz A 2012 *Physica* E **44** 1900
[17] Liu X, Zou L, Liu C, Zhang Z-H and Yuan J-H 2016 *Opt. Mater.* **53** 218
[18] Xie W 2014 *J. Lumin.* **145** 283
[19] Martınez-Orozco J C, Mora-Ramos M E and Duque C A 2012 *J. Lumin.* **132** 449
[20] Restrepo R L, Gonzalez-Pereira J P, Kasapoglu E, Morales A L and Duque C A 2018 *Opt. Mater.* **86** 590
[21] Baskoutas S, Paspalakis E and Terzis A F 2007 *J. Phys.: Condens. Matter* **19** 395024
[22] Eseanu N, Niculescu E C and Burileanu L M 2009 *Physica* E **41** 1386
[23] Lima F M S, Amato M A, Nunes O A C, Fonseca A L A, Enders B G and da Silva E F Jr 2009 *J. Appl. Phys.* **105** 123111
[24] Ozturk E 2010 *Eur. Phys. J.* B **75** 197
[25] Niculescu E C and Burileanu L M 2010 *Eur. Phys. J.* B **74** 117
[26] Ozturk O, Ozturk E and Elagoz S 2019 *Laser Phys.* **29** 055402

[27] Ozturk E and Sokmen I 2015 *Int. J. Mod. Phys.* B **29** 1550030
[28] Zhao G J, Liang X X and Ban S L 2003 *Phys. Lett.* A **319** 191
[29] Ozturk E 2014 *Opt. Commun.* **332** 136
[30] Peter A J and Navaneethakrishnan K 2008 *Superlattices Microstruct.* **43** 63
[31] Ozturk E and Sokmen I 2013 *J. Lumin.* **134** 42
[32] Pont M, Walet N R, Gavrila M and McCurdy C W 1998 *Phys. Rev. Lett.* **61** 939
[33] Zhang C 2001 *Appl. Phys. Lett.* **78** 4187
[34] Niculescu E C 2017 *Opt. Mater.* **64** 540
[35] Ozturk E 2016 *Laser Phys.* **26** 096102